HHS Public Access

Author manuscript

J Am Coll Cardiol. Author manuscript; available in PMC 2018 September 26.

Published in final edited form as:

J Am Coll Cardiol. 2017 September 26; 70(13): 1601–1615. doi:10.1016/j.jacc.2017.07.789.

Bone Marrow-derived Tenascin-C Attenuates Cardiac Hypertrophy by Controlling Inflammation

Lei Song, MD, **Lai Wang, MD**, **Fuqiang Li, PhD**, **Ada Yukht, MS**, **Minghui Qin, PhD**, **Haley Ruther, MS**, **Mingjie Yang, PhD**, **Aurelio Chaux, MD**, **Prediman K. Shah, MD**, and **Behrooz G. Sharifi, PhD**

Oppenheimer Atherosclerosis Research Center, Cedars Sinai Heart Institute, Los Angeles, California

Abstract

BACKGROUND—Tenascin-C (TNC) is a highly conserved matricellular protein with a distinct expression pattern during development and disease. Remodeling of the left ventricle (LV) in response to pressure overload leads to the re-expression of the fetal gene program.

OBJECTIVES—The aim of this study was to investigate the function of TNC in cardiac hypertrophy in response to pressure overload.

METHODS—Pressure overload was induced in TNC knockout and wild-type mice by constricting their abdominal aorta or infusion of angiotensin II. Echocardiography, immunostaining, flow cytometry, quantitative real-time polymerase chain reaction, and reciprocal bone marrow transplantation were used to evaluate the effect of TNC deficiency.

RESULTS—Echocardiographic analysis of pressure overloaded hearts revealed that all LV parameters (LV end-diastolic and end-systolic dimensions, ejection fraction, and fractional shortening) deteriorated in TNC-deficient mice compared to their wild-type counterparts. The size of cardiomyocytes and collagen accumulation were significantly higher in the absence of TNC. Mechanistically, TNC deficiency promoted rapid accumulation of the $CCR2^{+}/Ly6C^{hi}$ monocyte/macrophage subset into the myocardium in response to pressure overload. Further, echocardiographic and immunohistochemical analyses of recipient hearts showed that expression of TNC in the bone marrow, but not the myocardium, protected the myocardium against excessive remodeling of the pressure-overloaded heart.

CONCLUSIONS—TNC deficiency further impaired cardiac function in response to pressure overload and exacerbated fibrosis by enhancing inflammation. In addition, expression of TNC in the bone marrow, but not the myocardium, protected the myocardium against excessive remodeling in response to mild pressure overload.

Correspondence: Behrooz G. Sharifi, PhD, Oppenheimer Atherosclerosis Research Center, Division of Cardiology, Cedar-Sinai Heart Institute, Cedar-Sinai Medical Center, 8700 Beverly Boulevard, Davis Bldg. #1016, Los Angeles, California 90048, Telephone: (310) 423-7621, Fax: (310) 423-0922, Sharifi@cshs.org.

Disclosure statement: Nothing to disclose

Keywords

left ventricle; macrophage; monocyte; pressure overload

Introduction

Left ventricular hypertrophy (LVH) is a strong predictor of adverse cardiovascular outcomes and an important risk factor for sudden death and heart failure (1). LVH is a complex and multifactorial condition whose pathogenesis might include many different genetic and signaling pathways (2). At the cellular level, LVH is characterized by an increase in cell size, enhanced protein synthesis, and heightened organization of the sarcomere. At the molecular level, these changes in cellular phenotype are accompanied by the re-expression of fetal gene program (3).

Tenascin-C (TNC) is a member of matricellular proteins with distinct spatial and temporal expression during development, tissue homeostasis, and disease (4). It is highly expressed during fetal development but its expression is downregulated in adult tissues. Multiple functions have been attributed to TNC based upon its effects observed in cell culture and its distribution in tissues undergoing active restructuring. In different experimental models and tissues, TNC has been reported to mediate or inhibit cell adhesion (5–9), induce or inhibit differentiation (10,11), stimulate cell growth and survival (12,13), and promote apoptosis (14,15). Nonetheless, TNC's actions in the pathophysiology of cardiovascular disease in vivo remain uncertain.

The heart of TNC knock-out (TNCKO) mice develop normally and show no sign of deficiency (16–18). However, TNC is re-expressed in the myocardium in response to a wide array of cardiac injuries. This study aimed to investigate the significance of myocardial expression of TNC in the pathology of the pressure-overloaded heart.

Methods

All surgical procedures described were performed in accordance with the National Institute of Health standards and approved by the Institutional Animal Care and Use Committee of Cedars-Sinai Medical Center.

A more detailed methods section for this study is in the Online Appendix. Briefly, we used C57BL/6 (wild-type) mice (The Jackson Laboratory, Bar Harbor, Maine) as well as TNCKO mice (in the C57BL/6 background) from established colonies at Cedars-Sinai as previously described (19). Sex- and age-matched animals were used for all experiments. For experiments described in this publication adult male mice (11 to 12 weeks old) were used. At this age, developmental growth of the heart is complete. The weight of each mouse at this age ranged between 25 and 30 g. The number of mice used in each study is described in the tables and figure legends.

The mice groups were randomly selected for transverse aortic constriction (TAC) surgery, which is generally performed by placing a band on either the ascending, transverse, or

descending portion of the aorta depending on study design (20,21). Constriction of the ascending aorta provides an extreme and more rapid overload on the left ventricle (LV), whereas abdominal aorta constriction is milder and leaves intact a larger portion of the circulation as a means of possible compensation (20,21). Abdominal aortic constriction allowed us to produce mild pressure overload compared to the widely used ascending aortic banding. All baseline data were collected before TAC. The surgical procedure was performed essentially as previously described (22) on anesthetized male mice. At the indicated times after constriction, cardiac function and blood pressure (BP) were measured. The mice were euthanized and their tissues harvested for further analysis.

Measurement and Analysis

Transthoracic echocardiography was performed on anesthetized animals, with measurement of: ejection fraction (EF); fractional shortening (FS); LV internal diameter diastolic (LVIDd); LV internal diameter systolic (LVIDs); posterior wall thickness diastolic (PWTd); and posterior wall thickness systolic (PWTs). Three consecutive cardiac cycles were analyzed and the average was used for data analysis. The time points were selected for echocardiographic studies: pre-TAC (baseline); 1 month; and 2 months post-TAC.

Blood pressure (BP) was measured using a tail cuff CODA 6 system. Thoracic BP proximal to the constricted site was calculated by adding tail BP to the Doppler-derived BP gradient across the constriction. Multiple recordings were performed to obtain the average data.

After weighing mice, hearts were dissected at the indicated times post-TAC or sham-operated surgery from mice of each genotype, rinsed in phosphate-buffered saline, and weighed. Hearts were cut in a cross section just below the level of the papillary muscle. The top half of the heart was formalin fixed and embedded in paraffin. Sections (5 μm) were prepared at 200 μm intervals. The sections were stained with hematoxylin and eosin for examination of gross appearance, whereas Masson’s Trichrome or Periodic acid-Schiff counterstained with hematoxylin (PAS-H) was employed to facilitate quantification of fibrosis and cardiomyocyte size, respectively. Cardiomyocyte hypertrophy was assessed by measuring the cross-sectional area of 100 cardiomyocytes per PAS-H stained in 10 randomly selected fields having nearly circular capillary profiles and centered nuclei in the LV free wall. Cardiac fibrosis was determined by calculating the percentage of Masson’s Trichrome stained area of interstitial fibrosis per total area of cardiac tissue. Histological images were analyzed and blinded measurements made by 2 independent observers.

Peripheral blood was collected and cell viability determined by incubating cells with fixable single-color dyes for 30 min at room temperature. Only singlet cells were analyzed, all doublets were excluded from the analysis by monitoring the side scatter-forward scatter pulse width channel.

Deoxyribonucleic acid was extracted from recipient hearts, and the genotype determined using primers specific to the lacZ-neo gene construct used to generate TNCKO mice. Amplification with primers yielded a 1132 kb fragment for wild-type (WT) and an 800 kb fragment in TNCKO mice.

Total ribonucleic acid (RNA) was extracted from the lower half of the LV using TRIzol. After DNAse treatment, 500 ng of total RNA were reverse transcribed and RNA primers for each gene were designed using the Primer3 software program. Gene expression was determined by quantitative polymerase chain reaction (qPCR). Glyceraldehyde 3-phosphate dehydrogenase (GAPDH) was used as an internal control for the results presented here. There were no significant differences between genetic background or treatment in GAPDH expression levels. Fold change in expression was calculated using the $2^{-\delta\delta X\rho}$ method with results represented as mean fold changes relative to sham-operated or GAPDH expression. In the PCR studies, we show a representative experiment that has been done in triplicate with 3animals used for each PCR experiment.

Reciprocal Bone Marrow Transplantation

Reciprocal bone marrow transplantation (BMT) was performed essentially as described previously (23). Briefly, bone marrow was collected from the femurs and tibias of 6- to 7-week-old male donor mice and injected into the tail vein of lethally-irradiated male recipients. Transplantation groups are as follows: 1) positive control, both the donor and recipient were wild-type mice (WT-WT); 2) negative control, both the donor and recipient were TNCKO mice (T-T); 3) wild-type mice were used as bone marrow donors and the recipients were TNCKO mice (WT-T); and 4) bone marrow donors were TNCKO mice and the recipient group were wild-type mice (T-WT). The engraftment of bone marrow was evaluated by qPCR using primers specific for the Y chromosome (23). The aortic constriction surgery was performed on recipient mice at 6 weeks post-BMT and cardiac function was assessed at 2 months post-TAC.

Angiotensin II Infusion

Animals were anesthetized with isoflurane in oxygen delivered by a precision vaporizer. When surgical levels of anesthesia were reached, a 1 to 23cm mid-scapular skin incision was made and a mini osmotic pump was inserted subcutaneously. The incision was closed using 6-0 silk sutures. Animals from each genotype were randomly assigned to receive angiotensin II (AT II) (0.83μg/kg/min) or a vehicle control of saline. The pumps remained in for 28 days during which the animals were provided food and water ad libitum and observed for signs of morbidity. Prior to euthanization, echocardiographic analysis was performed and BP measurements were taken via a noninvasive cuff system for a minimum of 3 consecutive measurements.

Statistical Analysis

Statistical analysis was performed using Prism 4.0 (GraphPad Software, Inc., La Jolla, California). Statistical significance within genetic backgrounds was determined by using the 2-tailed unpaired Student *t* test or nonparametric Mann-Whitney *U* test, whereas a 2-way analysis of variance or the Kruskal-Wallis test was used to determine statistical significance within treatment groups. All results were expressed as means ± SD and p value < 0.05 was considered statistically significant.

Results

To determine whether mild pressure overload leads to the induction of TNC, we extracted RNA from the LV from WT mice before, 3 days, and 7 days after TAC, and the expression of TNC was quantified by qPCR. Mild pressure overload was found to induce TNC expression in the myocardium of WT control mice (Online Figure 1). Echocardiographic analysis was used to assess the LV geometry and function in WT and TNCKO mice at baseline and 2 months after the TAC procedure (Online Figure 2). Morbidity was similar between the 2 mouse genotypes as was their cardiac function at baseline (Table 1). However, all the parameters that define cardiac hypertrophy or remodeling (ejection fraction, fractional shortening, LV internal diameter, posterior wall thickness, and heart-to-body weight and ventricular mass-to-body weight ratios) were significantly exacerbated in TNC-deficient mice (Table 1). Similarly, the expression level of cardiac hypertrophy markers (atrial natriuretic and B-type peptides) were significantly higher in TNCKO mice compared to control mice (Online Figure 3).

To determine whether TNC deficiency influenced BP, we measured BP proximal to the constriction site in the 2 mice genotypes (Online Figure 4). Both groups were hypertensive at 1 and 2 months post-TAC compared with baseline, but with no significant difference in BP found for these 2 groups before and after TAC. Similarly, no significant differences in the heart rate were detected at baseline or after TAC in the 2 mice genotypes (not shown).

Hearts harvested 2 months after TAC clearly showed that TNCKO hearts were significantly larger with a thicker posterior wall compared to control hearts (Figure 1A). Analysis of the size of cardiomyocytes revealed that TNC deficiency had no effect on size at baseline (not shown). However, within the TAC groups, TNCKO hearts had a significantly increased size of cardiomyocytes (Figure 1B). Quantitative analysis of Masson’s Trichrome stained sections indicated that the absence of TNC significantly increased interstitial as well as perivascular fibrosis compared to controls (Figure 1C). Immunohistochemical analysis of the sections for the presence of microvessel density (von Willebrand factor) showed no significant difference in capillary density before and after TAC in the LVs of the 2 mice genotypes (not shown).

Effects of TNC Deficiency

The development of fibrosis is associated with activation of monocytes and macrophages (24,25). To determine monocyte infiltration, LV sections from the 2 mice genotypes were stained for presence of macrophages. Before TAC, there were no significant differences in the density of macrophages between the 2 genotypes (not shown). Within the TAC groups, TNC deficiency led to a rapid accumulation (within 3 days post-TAC) of a large number of monocytes and macrophages, which remained elevated for 7 days, declining thereafter (Figure 2A). Quantification showed that the level of infiltrating monocytes was markedly higher in TNCKO mice compared to WT at all timepoints (Figure 2B). In TNCKO mice, the level of cell infiltration did not change between days 3 and 7 post-TAC; however, at 30 days post-TAC, cell infiltration was significantly reduced (compared to 7 days post-TAC) (Figure 2B). In WT mice, a significant accumulation of monocytes ($p = 0.0001$) was detected at 7 days post-TAC compared with 3 days (Figure 2B). The infiltration level significantly

dropped at 30 days post-TAC. Staining of sections with anti-CD4 antibody showed few scattered $CD4^+$ cells present in the LV of both mouse genotypes after TAC, and absence of TNC did not significantly influence the level of $CD4^+$ cells (not shown).

To analyze the profile of monocyte/macrophage subsets in the LV of the 2 mice genotypes, LVs were harvested, weighed, digested with an enzyme cocktail, and the phenotype of monocytes and macrophages was determined by flow cytometry 7 days post-TAC. We used this early timepoint to identify the cell subsets that are most proximal to the initiating stimuli for cardiac hypertrophy and to minimize the contributions of operation-related events and phenomena secondary to the initial and essential cellular events that induce hypertrophy. (The strategy used for flow cytometry following LV digestion is shown in Online Figure 5).

Cumulative flow cytometry analyses of digested LVs from 5 mice per genotype showed that the frequency of neutrophil ($CD45^+$, $CD11b^+$, and $Ly6G^+$) infiltration was low in the 2 mice genotypes before TAC and the level of cells did not significantly change at 7 days post-TAC (Figure 3). The level of monocytes and macrophages ($CD45^+$, $CD11b^+$, and $Ly6G^-$) in the LV from the 2 mice genotypes were similar under basal conditions; however, the number of total monocytes and macrophages was significantly higher in the absence of TNC compared to the control ($p = 0.001$). Analysis of the monocyte/macrophage subtypes showed that the frequency of $CCR2^+$ ($p = 0.0004$) and $Ly6C^{hi}$ ($p = 0.001$) subsets were significantly higher in TNC-deficient mice compared to control mice using one-way analysis of variance analysis (Figure 3). Similarly, significant differences in the total number of monocytes and macrophages as well as their subsets were detected when we used the Student *t* test to compare TNCKO and WT left ventricles. These results suggested that while TNC deficiency had no effect on the pool of resident macrophages under basal conditions, absence of this protein led to a significant LV accumulation of the $CCR2^+$-$Ly6C^{hi}$ monocyte-macrophage subset in response to mild pressure overload.

Reciprocal BMT

In the TNCKO mouse, the heart develops normally and displays no obvious developmental defects (16–18). This occurs in the absence of compensation by other members of the tenascin family of proteins (16,26). In the adult heart, TNC is not expressed under basal conditions (18). Collectively these data suggest that TNC is not required for the development and normal function of the heart; yet, this protein is re-expressed in response to numerous cardiac injuries. It is thought that the re-expression of TNC exacerbates cardiac diseases (27,28); however, it is unclear why such negative activity of TNC on cardiac function was not observed during heart development and the heart of TNCKO mice function normally. We found that absence of TNC further impairs cardiac function and exacerbates inflammation and fibrosis, suggesting that TNC protects the myocardium against excessive remodeling. To determine the contribution of TNC to cardiac hypertrophy, we performed reciprocal BMT, where bone marrow from TNCKO mice was replaced with bone marrow from WT mice and vice versa, generating 2 chimeric mouse lines. The first chimeric group (T-WT, TNCKO donor to wild-type recipient) lacked the ability to express TNC in the bone marrow while cardiac cells remained competent to express TNC. The second chimeric group (WT-T, wild-type donor to TNCKO recipient) lacked the ability to express TNC in cardiac cells, while the

bone marrow became competent to express the protein. Two types of controls were used to account for the effect of total body irradiation on cardiac function (29); the positive control group (WT-WT, WT donor and recipient) and the negative control group (T-T, TNCKO donor and recipient). Chimerism was established in all recipient groups 1 month after BMT and all mouse groups were subjected to TAC for 2 months, at which time cardiac function was evaluated. The hearts were harvested and analyzed by immunostaining.

Analysis of cardiac function (ejection fraction, fractional shortening, end-diastolic volume, and end-systolic volume) showed no significant difference among the recipient groups before TAC (Online Figure 6). This suggested that TNC is not required for normal heart function, consistent with other reports (16–18). Within the TAC control groups, cardiac function of the negative control was significantly lower than the positive control (Figure 4), suggesting that TNC expression has protective activity, consistent with the results shown in (Table 1). Among the chimeric groups, cardiac function of the WT-T group significantly improved compared to the negative control group, reaching levels similar to the positive control group. In contrast, cardiac function of the T-WT group declined, reaching levels similar to the negative control group (Figure 4). Thus, bone marrow from a WT donor fully rescued the phenotype (i.e., cardiac function) of a TNCKO recipient despite the lack of TNC expression in the myocardium (as discussed later). In contrast, bone marrow from a TNCKO donor led to deterioration in cardiac function of WT recipient mice despite their ability to express TNC. The results are summarized in Table 2.

Following functional analysis, hearts were harvested and their weight-to-body-weight and heart-volume-to-body-weight ratios were determined (Figures 5A and 5B). The results paralleled those of echocardiographic analysis of cardiac function described above; that is, the ratios significantly improved in the WT-T group, reaching levels like the positive control, while the ratios for the T-WT group worsened, reaching levels similar to the negative control.

The results of immunohistochemical analysis of sections from the harvested recipient LVs were consistent with these data. Analysis of collagen accumulation revealed that the T-T and T-WT groups had the highest level of collagen compared with to the WT-T and WT-WT groups (Figure 5C). When the sections were stained for the expression of periostin, a surrogate for fibroblasts, the accumulation of fibroblasts was higher among the T-T and T-WT groups compared with the WT-T and WT-WT groups (Figure 5C).

Next, we determined the profile of TNC expression in the recipient LVs. Total RNA was isolated and TNC expression was analyzed by qPCR (Figure 5D). The 1,132 bp band, which is a surrogate for TNC expression, was not detectable in either TNCKO recipient group, suggesting that TNC is not expressed in the LV of these mice. In contrast, the 1,132 bp TNC band was detectable in the WT recipient groups, suggesting that the myocardium from these mice remained competent to express TNC after BMT. Additionally, these results suggested that the BMT did not alter the expression pattern of TNC in the myocardium of WT-recipient mice. Collectively, these results demonstrated that TNC expression in the myocardium of the T-WT chimeric group did not lead to the improvement of cardiac

function and hypertrophy when compared to the WT-T group, which did not express TNC in the myocardium.

Angiotensin II Infusion

Recently, investigators demonstrated that infusion of AT II has no effect on cardiac hypertrophy but stimulates cardiac fibrosis in TNCKO mice (7). In contrast, using abdominal aortic constriction, we noted that TNC deficiency exacerbated both cardiac hypertrophy and fibrosis. To determine whether these divergent results were related to the differences in the methodology to induce pressure overload or to other factors, animals were infused with AT II (800 ng/kg/min) or saline for 28 days, then cardiac function and wall thickness were measured by echocardiography. Hearts were harvested, weighed, and processed for analysis. While parameters that define cardiac hypertrophy were elevated in the 2 mice genotypes in response to AT II infusion, TNC deficiency led to a progressive increase in diastolic posterior wall thickness and LV systolic dimension, and the percentage of LV fractional shortening decreased progressively at 4 weeks compared to the control (Table 3).

Analysis of the harvested hearts showed that while infusion of AT II resulted in a significant increase in the whole-heart-mass-to-body-weight ratio in the 2 mice genotypes, the lack of TNC significantly increased the ratios ($p < 0.0001$) (Figure 6A). We next examined the extent of cardiac histopathology in the 4 experimental groups. Sections from WT and TNCKO mice were examined for extent of fibrosis (collagen deposition) and fibroblast accumulation. Among the AT II-infused groups, we noted a significant increase in the level of collagen deposition in the absence of TNC compared to controls (Figures 6B and 6C). Immunostaining of sections for the presence of fibroblasts showed that the frequency of the fibroblasts was higher in the TNC-deficient mice compared to controls (Figure 6D). Collectively, these data suggested that TNC deficiency exacerbates cardiac hypertrophy induced by infusion of AT II.

Discussion

In this paper, we analyzed the role of TNC in cardiac hypertrophy in response to mild pressure overload using TNCKO and WT mice (Central Illustration). Echocardiographic analysis revealed that cardiac function of WT mice was similar to those of TNCKO mice, suggesting that TNC is not required for normal function of the heart. Induction of mild pressure overload induced cardiac hypertrophy in both mice genotypes; however, the effect was significantly exacerbated in TNCKO mice. In line with echocardiographic analysis, hearts harvested 2 months post-TAC from TNCKO mice were significantly larger with a thicker posterior wall compared to hearts harvested from control mice. Similarly, the size of cardiomyocytes was larger in TNCKO hearts compared to control hearts and cardiac fibrosis was also significantly higher in hearts harvested from TNCKO mice. Thus, all the parameters that define cardiac hypertrophy are exacerbated in TNCKO compared to WT mice.

Immunostaining of heart sections from the 2 mouse genotypes showed that while there was no difference in the level of resident macrophages under basal conditions, mild pressure

overload significantly impacted the infiltration of monocytes, especially in TNCKO mice. The infiltration of a large number of monocytes was detected as early as 3 days following TAC, remained high at 7 days, and significantly declined at 30 days post-TAC in TNCKO mice. For WT mice, a significant infiltration of monocytes was observed at 7 days following TAC, returning to basal control levels at 30 days post-TAC. In line with the immunostaining data, flow cytometry analysis of LVs digested from the 2 mice genotypes showed that large numbers of $Ly6C^{hi}$ monocytes infiltrated into the myocardium of TNCKO mice in response to mild pressure. Expression of $Ly6C^{hi}$ has been considered as a signature of monocytes in extravascular tissues (30), suggesting that the cells likely originated from external sources rather than proliferation of local macrophages found in the myocardium. Similarly, we noted that the infiltrating cells also express a high level of CCR2. The $CCR2^{+}$-$Ly6C^{hi}$ monocyte possess a higher capacity to drive proinflammatory responses compared to other subsets (31,32), suggesting that lack of TNC increases the proinflammatory state of the myocardium in response to pressure overload compared to WT mice. Overall, TNC deficiency increased the proinflammatory state of the heart, leading to excessive remolding of the myocardium in response to mild pressure overload.

Both pro- and anti-inflammatory roles are reported for TNC. For example, TNC is thought to promote inflammation by acting as an endogenous activator of innate immunity (33) while others suggest that the rapid production of TNC in inflamed tissues is required to control the spread of inflammation (34). In support of the anti-inflammatory role of TNC, in vitro studies have shown that TNC production is induced by anti-inflammatory cytokines (35–37), TNC inhibits T cell activation (38), and myeloid cells fail to effectively migrate through a matrix barrier containing TNC (39). In vivo studies have demonstrated that TNC deficiency aggregated experimental dermatitis and nephritis (40,41). Furthermore, TNC was found to suppress the immune response in the brain by blocking T cell migration (42). Finally, increased numbers of monocytes and macrophages were found in the tumor stroma of spontaneously arising mammary tumors in the absence of TNC compared to TNC sufficient stroma (43). Our data supported the anti-inflammatory role for TNC in vivo.

The heart of a TNC-null mouse develops normally and displays no obvious developmental defects (16–18). In addition, other members of the tenascin family do not compensate for the absence of the TNC gene (16,26). In the adult heart, TNC is not expressed under basal conditions (18). Together, these data suggest that TNC is not required for either the development of the heart or its normal function; yet, this protein is re-expressed in the heart in response to a wide variety of cardiac injuries. Results of the reciprocal BMT indicated that expression of TNC in the heart is not relevant to its function. In the T-T group, cardiac function was significantly impaired compared to the WT-WT group, suggesting that global expression of TNC improves function of the pressure overloaded heart. Analysis of TNC expression in the WT-T group showed that while TNC is not expressed in the myocardium, all the parameters that define cardiac hypertrophy and fibrosis were improved compared to the negative control group (T-T). Conversely, despite expression of TNC in the heart of the T-WT group, cardiac hypertrophy deteriorated compared with the positive control group (WT-WT). Collectively, these results strongly demonstrated that TNC expression in the heart is irrelevant to its function in response to mild pressure overload. In addition, these results underscore the significant contribution of bone marrow to cardiac hypertrophy, in this case

the ability of bone marrow to express TNC. Other studies also highlighted the significant contribution of the bone marrow to cardiac hypertrophy. For example, lack of B7 ligands blunted hypertension in response to both AT II and deoxycorticosterone acetate salt challenges, and transplantation of bone marrow to these animals restores their BP elevation (44). This and other studies (45–47), together with our data, point to the pivotal role of bone marrow in the development of cardiac hypertrophy.

The role of TNC in cardiac pathologies is poorly defined. We used abdominal aortic constriction and AT II infusion approaches to induce mild pressure overload and both methodologies led to a similar conclusion: TNC protects the myocardium against excessive remodeling in response to pressure overload. In contrast, infusion of AT II in TNCKO mice was reported to attenuate cardiac fibrosis without having any effect on cardiac hypertrophy (7). Given the intimate connection between fibrosis and cardiac hypertrophy (48–50), it remains unclear why cardiac hypertrophy was unaffected while fibrosis was attenuated in TNCKO mice. While the reason for the inconsistency between our results and the published data is unknown, differences in the methodologies to induce pressure overload most likely do not account for the discrepancy. We speculate that differences in the genetic background of the TNCKO mouse might in part contribute to this inconsistency. In our study, TNCKO mice were established in the C57BL/6 background versus the BALB/c background of TNCKO mice used in reported cases of cardiac disease (7,51–54). The genetic background plays a key role in cardiac pathologies. For example, unlike other strains of mice, C57BL/6 mice develop rapid LV dilation (55,56), and infarct rupture is more frequent in C57BL/6 mice compared to BALB/c mice (57). In addition, C57BL/6 mice are more prone to the development of atherosclerosis compared to BALB/c mice (58,59). These differences in cardiac pathologies may, in part, be related to the immune response among different mouse strains. For instance, BALB/c mice predominantly exhibit Th2 responses whereas C57BL/6 mice display Th1 dominant responses to the same antigen (60,61). Also, the innate immune response is highly influenced by the genetic background of the mouse (62). Given the importance of proinflammatory signaling in cardiac pathologies and LV remodeling (63–65), mouse strains with the impaired Th1/M1 immune response (e.g., BALB/c) may not be a suitable animal model to study cardiovascular diseases.

Study Limitations

Although this study was performed using C57BL/6 mouse which displays the dominant Th1/M1 response, the results cannot be extended to other strains of mice with the dominant Th2/M2 response.

Conclusions

This study added clarification to the confusing and seemingly contradictory information concerning the role of TNC in the remodeling of cardiac tissue. We found that TNC deficiency led to the deterioration and excessive remodeling of the LV in response to mild pressure overload. This deterioration was associated with increased fibrosis and infiltration of proinflammatory monocyte subsets into the myocardium. Reciprocal BMT studies showed that lack of TNC expression in the bone marrow, but not in the myocardium, is

responsible for the deterioration of cardiac function in TNCKO mice. The transient nature of TNC re-expression, together with our data, suggest that lack of TNC activity during tissue regeneration and/or remodeling might have repercussions associated with the exacerbation of cardiac pathology.

METHODS

All surgical procedures described were performed in accordance with the National Institute of Health standards and approved by the Institutional Animal Care and Use Committee of Cedars-Sinai Medical Center.

Briefly, we used C57BL/6 (wild-type) mice (The Jackson Laboratory, Bar Harbor, Maine) as well as TNCKO mice (in the C57BL/6 background) from established colonies at Cedars-Sinai as previously described (19). Sex- and age-matched animals were used for all experiments. For experiments described in this publication adult male mice (11 to 12 weeks old) were used. At this age, developmental growth of the heart is complete. The weight of each mouse at this age ranged between 25 and 30 g. The number of mice used in each study is described in the tables and figure legends.

The mice groups were randomly selected for transverse aortic constriction (TAC) surgery, which is generally performed by placing a band on either the ascending, transverse, or descending portion of the aorta depending on study design (20,21). Constriction of the ascending aorta provides an extreme and more rapid overload on the left ventricle (LV), whereas abdominal aorta constriction is milder and leaves intact a larger portion of the circulation as a means of possible compensation (20,21). Abdominal aortic constriction allowed us to produce mild pressure overload compared to the widely used ascending aortic banding. All baseline data were collected before TAC. The surgical procedure was performed essentially as previously described (22) on anesthetized male mice (11 to 12 weeks old). were anesthetized with Ketamine-Xylazine by intraperitoneal injection. The abdomen was opened and the abdominal aorta at the suprarenal level was freed of the surrounding adventitial adipose tissue by careful dissection. The aorta was constricted by 9-0 silk sutures that were placed around the aorta and a 28 g needle was placed between the celiac and superior mesenteric arteries followed by a double surgeon’s knot that secured the suture around the aorta and needle. The needle was removed resulting in a 33% narrowing of the luminal diameter (23). At the indicated times after constriction, cardiac function and blood pressure (BP) were measured. The mice were euthanized and their tissues harvested for further analysis.

MEASUREMENT AND ANALYSIS

Transthoracic echocardiography was performed on anesthetized animals, by isoflurane (2% induction and 1.5% maintenance). Two-dimensional short and long-axis images of the left ventricle were obtained at the papillary muscle level. The following parameters were measured: ejection fraction (EF); fractional shortening (FS); LV internal diameter diastolic (LVIDd); LV internal diameter systolic (LVIDs); posterior wall thickness diastolic (PWTd); and posterior wall thickness systolic (PWTs). Three consecutive cardiac cycles were

analyzed and the average was used for data analysis. The time points were selected for echocardiographic studies: pre-TAC (baseline); 1 month; and 2 months post-TAC.

Blood pressure (BP) was measured using a tail cuff CODA 6 system. Thoracic BP proximal to the constricted site was calculated by adding tail BP to the Doppler-derived BP gradient across the constriction. Multiple recordings were performed to obtain the average data.

After weighing mice, hearts were dissected at the indicated times post-TAC or sham-operated surgery from mice of each genotype, rinsed in phosphate-buffered saline, and weighed. Hearts were cut in a cross section just below the level of the papillary muscle. The top half of the heart was formalin fixed and embedded in paraffin. Sections (5 μm) were prepared at 200 μm intervals. The sections were stained with hematoxylin and eosin for examination of gross appearance, whereas Masson's Trichrome or Periodic acid-Schiff counterstained with hematoxylin (PAS-H) was employed to facilitate quantification of fibrosis and cardiomyocyte size, respectively. Cardiomyocyte hypertrophy was assessed by measuring the cross-sectional area of 100 cardiomyocytes per PAS-H stained in 10 randomly selected fields having nearly circular capillary profiles and centered nuclei in the LV free wall. Cardiac fibrosis was determined by calculating the percentage of Masson's Trichrome stained area of interstitial fibrosis per total area of cardiac tissue. Inflammatory cells were detected by using rat anti-mouse monoclonal immunoglobulin G (IgG) macrophage/monocyte marker (Mac-2; CEDARLANE, Burlington, Canada) followed by biotinylated rabbit anti-rat IgG with visualization using the ABC Elite Kit (Vector Laboratories, Burlingame, California). Positively stained cells per cross section were manually counted in 3 sections per heart. Endothelial cells were stained with the rabbit anti-Von Willebrand Factor antibody (Dako North America, Carpinteria, California), and fibroblasts were stained with the goat anti-periostin antibody (Santa Cruz Biotechnology, Dallas, Texas). Histologic images were analyzed by ImagePro version 4.1 and blinded measurements made by 2 independent observers.

Peripheral blood was collected by retro-orbital venous sinus sampling using heparin-coated tubes. Erythrocytes were lysed using a red blood cell lysis buffer. Hearts were extensively flushed with phosphate-buffered saline and then LVs were excised, minced with scissors, and digested in collagenase I (450 U/ml), collagenase XI (125 U/ml), DNase I (60 U/ml), and hyaluronidase (60 U/ml) at 37°C for 1 h. LVs were subsequently filtered through a 40-μm cell strainer.and cell viability determined by incubating cells with fixable single-color dyes for 30 min at room temperature. After 1 rinse with washing buffer, cells were incubated with CD16/32 antibody (Biolegend, San Diego, California) at 4°C for 15 min to block nonspecific binding. Cells were then labeled with the following rat anti-mouse antibodies (Biolegend): PE-labeled anti-CD45, PE-Cy7 labeled anti-CD11b, Brilliant Violet 421 labeled anti-F4/80, and PerCP-Cy5.5 labeled anti-Ly6G. Cells were also labeled with the Alexa Fluor 700 labeled anti-Ly6C (BD Biosciences, San Diego, California) and APC labeled anti-CCR2 (R&D Systems, Inc., Minneapolis, Minnesota). Cells were washed twice, resuspended in staining buffer, and immediately recorded with Becton Dickinson LSR Fortessa (BD Biosciences) at the Flow Cytometry Core of Cedars-Sinai Medical Center. Data were analyzed with Summit V4.3.Only singlet cells were analyzed, all doublets were

excluded from the analysis by monitoring the side scatter-forward scatter pulse width channel.

Deoxyribonucleic acid was extracted from recipient hearts using DNeasy Blood & Tissue Kit (Qiagen Science Inc., Germantown, Maryland), and the genotype determined using primers specific to the lacZ/neo gene construct used to generate TNCKO mice. Amplification with primers yielded a 1132 kb fragment for wild-type (WT) and an 800 kb fragment in TNCKO mice.

Total ribonucleic acid (RNA) was extracted from the lower half of the LV using TRIzol. After DNAse treatment, 500 ng of total RNA were reverse transcribed using the High-Capacity cDNA Archive Kit (Applied Biosystems) and RNA primers for each gene were designed using the Primer3 software program. Gene expression was determined by quantitative polymerase chain reaction (qPCR). using SsoFast EvaGreen Supermix (Bio-Rad Laboratories, Hercules, California). Glyceraldehyde 3-phosphate dehydrogenase (GAPDH) was used as an internal control for the results presented here. There were no significant differences between genetic background or treatment in GAPDH expression levels. Reactions were run on a iQ5 machine (BioRad) with analysis software. Threshold cycles were determined by an in-program algorithm assigning a fluorescence baseline based on readings before exponential amplification. Fold change in expression was calculated using the $2^{-\delta\delta X\rho}$ method with results represented as mean fold changes relative to sham-operated or GAPDH expression. In the PCR studies, we show a representative experiment that has been done in triplicate with 3animals used for each PCR experiment.

RECIPROCAL BONE MARROW TRANSPLANTATION

Reciprocal bone marrow transplantation (BMT) was performed essentially as described previously (24). Briefly, bone marrow was collected from the femurs and tibias of 6- to 7-week-old male donor mice and injected into the tail vein of lethally-irradiated male recipients. Transplantation groups are as follows: 1) positive control, both the donor and recipient were wild-type mice (WT-WT); 2) negative control, both the donor and recipient were TNCKO mice (T-T); 3) wild-type mice were used as bone marrow donors and the recipients were TNCKO mice (WT-T); and 4) bone marrow donors were TNCKO mice and the recipient group were wild-type mice (T-WT). The engraftment of bone marrow was evaluated by qPCR using primers specific for the Y chromosome (24). The aortic constriction surgery was performed on recipient mice at 6 weeks post-BMT and cardiac function was assessed at 2 months post-TAC.

ANGIOTENSIN II INFUSION

Animals were anesthetized with isoflurane in oxygen delivered by a precision vaporizer. When surgical levels of anesthesia were reached, a 1 to 23cm mid-scapular skin incision was made and a mini osmotic pump was inserted subcutaneously. The incision was closed using 6-0 silk sutures. Animals from each genotype were randomly assigned to receive angiotensin II (AT II) (0.83μg/kg/min) or a vehicle control of saline. The pumps remained in for 28 days during which the animals were provided food and water ad libitum and observed for signs of morbidity. Prior to euthanization, echocardiographic analysis was performed and BP

measurements were taken via a noninvasive cuff system for a minimum of 3 consecutive measurements.

STATISTICAL ANALYSIS

Statistical analysis was performed using Prism 4.0 (GraphPad Software, Inc., La Jolla, California). Statistical significance within genetic backgrounds was determined by using the 2-tailed unpaired Student *t* test or non-parametric Mann-Whitney *U* test, whereas a 2-way analysis of variance or the Kruskal-Wallis test was used to determine statistical significance within treatment groups. All results were expressed as means ± SD and p value < 0.05 was considered statistically significant.

Supplementary Material

Refer to Web version on PubMed Central for supplementary material.

ABBREVIATIONS AND ACRONYMS

AT II	angiotensin II
LVH	left ventricular hypertrophy
PCR	polymerase chain reaction
qPCR	quantitative PCR
TAC	transverse aortic constriction
TNC	tenascin-C
TNCKO	tenascin-C knockout
WT	wild type

References

1. Frey N, Katus HA, Olson EN, Hill JA. Hypertrophy of the heart: a new therapeutic target? Circulation. 2004; 109:1580–9. [PubMed: 15066961]
2. Xie M, Burchfield JS, Hill JA. Pathological Ventricular Remodeling: Mechanisms: Part 1 of 2. Circulation. 2013; 128:388–400. [PubMed: 23877061]
3. Izumo S, Nadal-Ginard B, Mahdavi V. Protooncogene induction and reprogramming of cardiac gene expression produced by pressure overload. Proc Natl Acad Sci U S A. 1988; 85:339–43. [PubMed: 2963328]
4. Midwood KS, Orend G. The role of tenascin-C in tissue injury and tumorigenesis. J Cell Commun Signal. 2009; 3:287–310. [PubMed: 19838819]
5. Grumet M, Milev P, Sakurai T, et al. Interactions with tenascin and differential effects on cell adhesion of neurocan and phosphacan, two major chondroitin sulfate proteoglycans of nervous tissue. J Biol Chem. 1994; 269:12142–6. [PubMed: 7512960]
6. LaFleur DW, Chiang J, Fagin JA, et al. Aortic smooth muscle cells interact with tenascin-C through its fibrinogen-like domain. J Biol Chem. 1997; 272:32798–803. [PubMed: 9407055]
7. Shimojo N, Hashizume R, Kanayama K, et al. Tenascin-C May Accelerate Cardiac Fibrosis by Activating Macrophages via the Integrin αVβ3/Nuclear Factor–κ B/Interleukin-6 Axis. Hypertension. 2015; 66:757–66. [PubMed: 26238448]

8. Chiquet-Ehrismann R, Kalla P, Pearson CA, Beck K, Chiquet M. Tenascin interferes with fibronectin action. Cell. 1988; 53:383–90. [PubMed: 2452695]
9. LaFleur DW, Fagin JA, Forrester JS, Rubin SA, Sharifi BG. Cloning and characterization of alternatively spliced isoforms of rat tenascin. Platelet-derived growth factor-BB markedly stimulates expression of spliced variants of tenascin mRNA in arterial smooth muscle cells. J Biol Chem. 1994; 269:20757–63. [PubMed: 7519614]
10. Mackie EJ, Tucker RP, Halfter W, Chiquet-Ehrismann R, Epperlein HH. The distribution of tenascin coincides with pathways of neural crest cell migration. Ann N Y Acad Sci. 1988; 540:64–77. [PubMed: 2462837]
11. Crossin KL, Hoffman S. Expression of adhesion molecules during the formation and differentiation of the avian endocardial cushion tissue. Dev Biol. 1991; 145:277–86. [PubMed: 1710192]
12. Jones PL, Cowan KN, Rabinovitch M. Tenascin-C, proliferation and subendothelial fibronectin in progressive pulmonary vascular disease. Am J Pathol. 1997; 150:1349–60. [PubMed: 9094991]
13. Jones PL, Crack J, Rabinovitch M. Regulation of tenascin-C, a vascular smooth muscle cell survival factor that interacts with the alphavbeta3 integrin to promote epidermal growth factor receptor phosphorylation and growth. J Cell Biol. 1997; 139:279–93. [PubMed: 9314546]
14. Boudreau N, Werb Z, Bissell MJ. Suppression of apoptosis by basement membrane requires three-dimensional tissue organization and withdrawal from the cell cycle. Proc Natl Acad Sci U S A. 1996; 93:3509–13. [PubMed: 8622967]
15. Wallner K, Li C, Shah PK, Wu K-J, Schwartz SM, Sharifi BG. EGF-Like Domain of Tenascin-C Is Proapoptotic for Cultured Smooth Muscle Cells. Arterioscler Thromb Vasc Biol. 2004; 24:1416–21. [PubMed: 15178565]
16. Saga Y, Yagi T, Ikawa Y, Sakakura T, Aizawa S. Mice develop normally without tenascin. Genes Dev. 1992; 6:1821–31. [PubMed: 1383086]
17. Forsberg E, Hirsch E, Frohlich L, et al. Skin wounds and severed nerves heal normally in mice lacking tenascin-C. Proc Natl Acad Sci U S A. 1996; 93:6594–9. [PubMed: 8692862]
18. Imanaka-Yoshida K, Matsumoto K, Hara M, Sakakura T, Yoshida T. The dynamic expression of tenascin-C and tenascin-X during early heart development in the mouse. Differentiation. 2003; 71:291–8. [PubMed: 12823230]
19. Wang L, Wang W, Shah PK, Song L, Yang M, Sharifi BG. Deletion of tenascin-C gene exacerbates atherosclerosis and induces intraplaque hemorrhage in Apo-E-deficient mice. Cardiovasc Pathol. 2012; 21:398–413. [PubMed: 22300502]
20. deAlmeida AC, van Oort RJ, Wehrens XHT. Transverse Aortic Constriction in Mice. J Vis Exp. 2010 Apr 21.(38)doi: 10.3791/1729
21. Tarnavski O, McMullen JR, Schinke M, Nie Q, Kong S, Izumo S. Mouse cardiac surgery: comprehensive techniques for the generation of mouse models of human diseases and their application for genomic studies. Physiol Genomics. 2004; 16:349–60. [PubMed: 14679301]
22. Song L, Wang L, Shah PK, Chaux A, Sharifi BG. Bioengineered vascular graft grown in the mouse peritoneal cavity. J Vasc Surg. 2010; 52:994–1002. 1002.e1–2. [PubMed: 20692791]
23. Wang L, Sharifi BG, Pan T, Song L, Yukht A, Shah PK. Bone marrow transplantation shows superior atheroprotective effects of gene therapy with apolipoprotein A-I Milano compared with wild-type apolipoprotein A-I in hyperlipidemic mice. J Am Coll Cardiol. 2006; 48:1459–68. [PubMed: 17010811]
24. Wynn TA, Barron L. Macrophages: Master Regulators of Inflammation and Fibrosis. Seminars in liver disease. 2010; 30:245–57. [PubMed: 20665377]
25. Duffield JS, Lupher M, Thannickal VJ, Wynn TA. Host Responses in Tissue Repair and Fibrosis. Annu Rev Pathol. 2013; 8:241–76. [PubMed: 23092186]
26. Steindler DA, Settles D, Erickson HP, et al. Tenascin knockout mice: barrels, boundary molecules, and glial scars. J Neurosci. 1995; 15:1971–83. [PubMed: 7534342]
27. Golledge J, Clancy P, Maguire J, Lincz L, Koblar S. The role of tenascin C in cardiovascular disease. Cardiovasc Res. 2011; 92:19–28. [PubMed: 21712412]
28. Imanaka-Yoshida K. Tenascin-C in Cardiovascular Tissue Remodeling. Circulation. 2012; 76:2513–20.

29. Tapio S. Pathology and biology of radiation-induced cardiac disease. J Radiat Res. 2016; 57:439–48. [PubMed: 27422929]
30. Jakubzick C, Gautier EL, Gibbings SL, et al. Minimal differentiation of classical monocytes as they survey steady state tissues and transport antigen to lymph nodes. Immunity. 2013; 39:599–610. [PubMed: 24012416]
31. Epperlein HH, Halfter W, Tucker RP. The distribution of fibronectin and tenascin along migratory pathways of the neural crest in the trunk of amphibian embryos. Development. 1988; 103:743–56. [PubMed: 2470571]
32. Lavine KJ, Epelman S, Uchida K, et al. Distinct macrophage lineages contribute to disparate patterns of cardiac recovery and remodeling in the neonatal and adult heart. Proc Natl Acad Sci U S A. 2014; 111:16029–34. [PubMed: 25349429]
33. Midwood KS, Hussenet T, Langlois B, Orend G. Advances in tenascin-C biology. Cell Mol Life Sci. 2011; 68:3175–99. [PubMed: 21818551]
34. Chiquet-Ehrismann R, Chiquet M. Tenascins: regulation and putative functions during pathological stress. J Pathol. 2003; 200:488–99. [PubMed: 12845616]
35. Makhluf HA, Stepniakowska J, Hoffman S, Smith E, LeRoy EC, Trojanowska M. IL-4 upregulates tenascin synthesis in scleroderma and healthy skin fibroblasts. J Invest Dermatol. 1996; 107:856–9. [PubMed: 8941674]
36. Phipps S, Ying S, Wangoo A, Ong YE, Levi-Schaffer F, Kay AB. The relationship between allergen-induced tissue eosinophilia and markers of repair and remodeling in human atopic skin. J Immunol. 2002; 169:4604–12. [PubMed: 12370399]
37. Jinnin M, Ihn H, Asano Y, Yamane K, Trojanowska M, Tamaki K. Upregulation of Tenascin-C Expression by IL-13 in Human Dermal Fibroblasts via the Phosphoinositide 3-kinase/Akt and the Protein Kinase C Signaling Pathways. J Invest Dermatol. 2006; 126:551–60. [PubMed: 16374482]
38. Ruegg CR, Chiquet-Ehrismann R, Alkan SS. Tenascin, an extracellular matrix protein, exerts immunomodulatory activities. Proc Natl Acad Sci U S A. 1989; 86:7437–41. [PubMed: 2477841]
39. Loike JD, Cao L, Budhu S, Hoffman S, Silverstein SC. Blockade of alpha 5 beta 1 integrins reverses the inhibitory effect of tenascin on chemotaxis of human monocytes and polymorphonuclear leukocytes through three-dimensional gels of extracellular matrix proteins. J Immunol. 2001; 166:7534–42. [PubMed: 11390508]
40. Koyama Y, Kusubata M, Yoshiki A, et al. Effect of tenascin-C deficiency on chemically induced dermatitis in the mouse. J Invest Dermatol. 1998; 111:930–5. [PubMed: 9856798]
41. Nakao N, Hiraiwa N, Yoshiki A, Ike F, Kusakabe M. Tenascin-C promotes healing of Habu-snake venom-induced glomerulonephritis: studies in knockout congenic mice and in culture. Am J Pathol. 1998; 152:1237–45. [PubMed: 9588892]
42. Huang J-Y, Cheng Y-J, Lin Y-P, et al. Extracellular Matrix of Glioblastoma Inhibits Polarization and Transmigration of T Cells: The Role of Tenascin-C in Immune Suppression. J Immunol. 2010; 185:1450–9. [PubMed: 20622113]
43. Talts JF, Wirl G, Dictor M, Muller WJ, Fassler R. Tenascin-C modulates tumor stroma and monocyte/macrophage recruitment but not tumor growth or metastasis in a mouse strain with spontaneous mammary cancer. J Cell Sci. 1999; 112:1855–64. [PubMed: 10341205]
44. Vinh A, Chen W, Blinder Y, et al. Inhibition and Genetic Ablation of the B7/CD28 T-Cell Costimulation Axis Prevents Experimental Hypertension. Circulation. 2010; 122:2529–37. [PubMed: 21126972]
45. Santisteban MM, Ahmari N, Carvajal JM, et al. Involvement of Bone Marrow Cells and Neuroinflammation in Hypertension: Novelty and Significance. Circ Res. 2015; 117:178–91. [PubMed: 25963715]
46. Ahmari N, Schmidt JT, Krane GA, et al. Loss of bone marrow adrenergic beta 1 and 2 receptors modifies transcriptional networks, reduces circulating inflammatory factors, and regulates blood pressure. Physiol Genomics. 2016; 48:526–36. [PubMed: 27235450]
47. Li Y, Kinzenbaw DA, Modrick ML, Pewe LL, Faraci FM. Context-dependent effects of SOCS3 in angiotensin II-induced vascular dysfunction and hypertension in mice: mechanisms and role of bone marrow-derived cells. Am J Physiol Heart Circ Physiol. 2016; 311:H146–56. [PubMed: 27106041]

48. Weber KT, Brilla CG. Pathological hypertrophy and cardiac interstitium. Fibrosis and renin-angiotensin-aldosterone system. Circulation. 1991; 83:1849–65. [PubMed: 1828192]
49. Conrad CH, Brooks WW, Hayes JA, Sen S, Robinson KG, Bing OHL. Myocardial Fibrosis and Stiffness With Hypertrophy and Heart Failure in the Spontaneously Hypertensive Rat. Circulation. 1995; 91:161–70. [PubMed: 7805198]
50. Ho CY, López B, Coelho-Filho OR, et al. Myocardial Fibrosis as an Early Manifestation of Hypertrophic Cardiomyopathy. N Engl J Med. 2010; 363:552–63. [PubMed: 20818890]
51. Nishioka T, Onishi K, Shimojo N, et al. Tenascin-C may aggravate left ventricular remodeling and function after myocardial infarction in mice. Am J Physiol Heart Circ Physiol. 2010; 298:H1072–8. [PubMed: 20081106]
52. Sawada Y, Onoda K, Imanaka-Yoshida K, et al. Tenascin-C synthesized in both donor grafts and recipients accelerates artery graft stenosis. Cardiovasc Res. 2007; 74:366–76. [PubMed: 17383619]
53. Yamamoto K, Onoda K, Sawada Y, et al. Tenascin-C is an essential factor for neointimal hyperplasia after aortotomy in mice. Cardiovasc Res. 2005; 65:737–42. [PubMed: 15664401]
54. Tamaoki M, Imanaka-Yoshida K, Yokoyama K, et al. Tenascin-C regulates recruitment of myofibroblasts during tissue repair after myocardial injury. Am J Pathol. 2005; 167:71–80. [PubMed: 15972953]
55. Barrick CJ, Rojas M, Schoonhoven R, Smyth SS, Threadgill DW. Cardiac response to pressure overload in 129S1/SvImJ and C57BL/6J mice: temporal- and background-dependent development of concentric left ventricular hypertrophy. Am J Physiol Heart Circ Physiol. 2007; 292:H2119–30. [PubMed: 17172276]
56. Patten RD, Hall-Porter MR. Small Animal Models of Heart Failure: Development of Novel Therapies, Past and Present. Circ Heart Fail. 2009; 2:138–44. [PubMed: 19808329]
57. van den Borne SWM, van de Schans VAM, Strzelecka AE, et al. Mouse strain determines the outcome of wound healing after myocardial infarction. Cardiovasc Res. 2009; 84:273–82. [PubMed: 19542177]
58. Schulte S, Sukhova GK, Libby P. Genetically Programmed Biases in Th1 and Th2 Immune Responses Modulate Atherogenesis. Am J Pathol. 2008; 172:1500–8. [PubMed: 18467709]
59. Tabibiazar R, Wagner RA, Spin JM, et al. Mouse Strain–Specific Differences in Vascular Wall Gene Expression and Their Relationship to Vascular Disease. Arterioscler Thromb Vasc Biol. 2005; 25:302–8. [PubMed: 15550693]
60. Mosmann TR, Coffman RL. TH1 and TH2 cells: different patterns of lymphokine secretion lead to different functional properties. Annu Rev Immunol. 1989; 7:145–73. [PubMed: 2523712]
61. Watanabe H, Numata K, Ito T, Takagi K, Matsukawa A. Innate immune response in Th1- and Th2-dominant mouse strains. Shock. 2004; 22:460–6. [PubMed: 15489639]
62. Howes A, Taubert C, Blankley S, et al. Differential Production of Type I IFN Determines the Reciprocal Levels of IL-10 and Proinflammatory Cytokines Produced by C57BL/6 and BALB/c Macrophages. J Immunol. 2016; 197:2838–53. [PubMed: 27549173]
63. Fernandez-Ruiz I. Immune system and cardiovascular disease. Nat Rev Cardiol. 2016; 13:503.doi: 10.1038/nrcardio.2016.127 [PubMed: 27516069]
64. Meng X, Yang J, Dong M, et al. Regulatory T cells in cardiovascular diseases. Nat Rev Cardiol. 2016; 13:167–79. [PubMed: 26525543]
65. Nahrendorf M, Pittet MJ, Swirski FK. Monocytes: Protagonists of Infarct Inflammation and Repair After Myocardial Infarction. Circulation. 2010; 121:2437–45. [PubMed: 20530020]

Perspectives

COMPETENCY IN MEDICAL KNOWLEDGE

Recent studies have suggested that inflammation and fibrosis play an important role in contributing to maladaptive LV remodeling from pressure overload. This proinflammatory-profibrotic response might be favorably modulated by genes such as TNC, especially TNC expressed in bone marrow-derived cells.

TRANSLATIONAL OUTLOOK

Heart failure is a serious and common clinical problem. Maladaptive LV remodeling plays a role in the genesis of heart failure. Modulating inflammatory and profibrotic myocardial response by TNC has the potential to lead to novel anti-inflammatory interventions against heart failure.

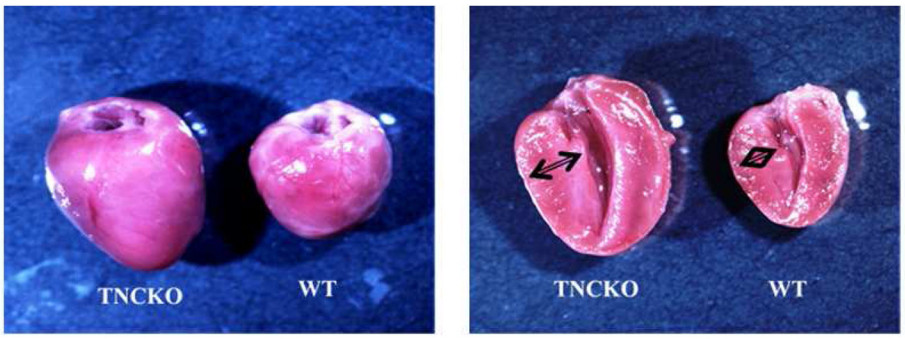

Fig. 1A

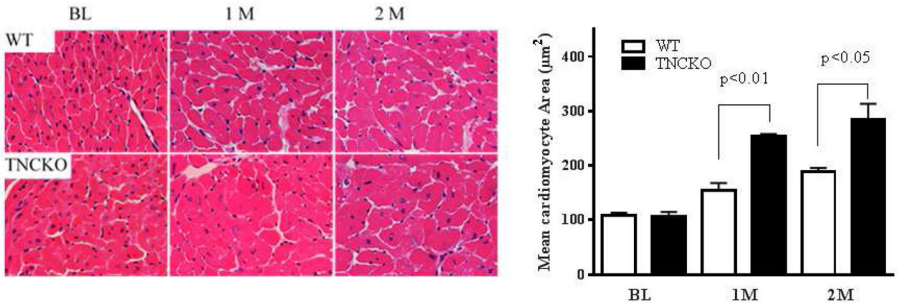

Fig. 1B

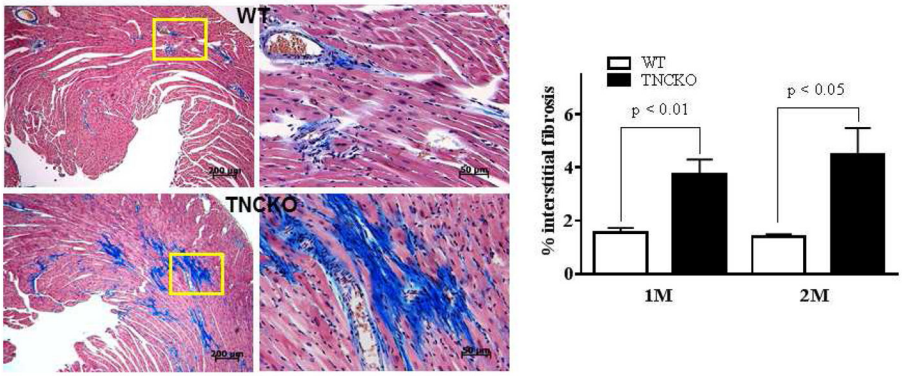

Fig. 1C

Figure 1. Effect of TNC Deficiency on Cardiac Hypertrophy

(A) Representative photographs of whole hearts harvested from the 2 mice genotypes demonstrated major differences in the heart size and posterior wall thickness at 2 months after surgery. **(B)** Representative histology of Periodic acid-Schiff counterstained with

hematoxylin-stained cardiac sections from the left ventricular (LV) septal wall of wild-type (WT) and tenascin-C knockout (TNCKO) mice at baseline (BL), 1 month, and 2 months post-transverse aortic constriction (TAC). In general, cardiomyocyte size was increased in TAC mice relative to BL. Within the TAC treatment group, the LV from TNCKO mice had the greatest increase in cardiomyocyte area compared to WT mice. Cardiomyocyte area is represented as mean ± SE. **(C)** In representative photomicrographs of heart sections stained with Masson Trichrome, (magnifications: 10X [left] and 40X [right]), there was no detectable fibrosis at BL between the 2 mice genotypes, but there was a significant difference in fibrosis within the TAC groups. Each cardiac section (in % interstitial fibrosis/mm^2) is represented as means ± SE.

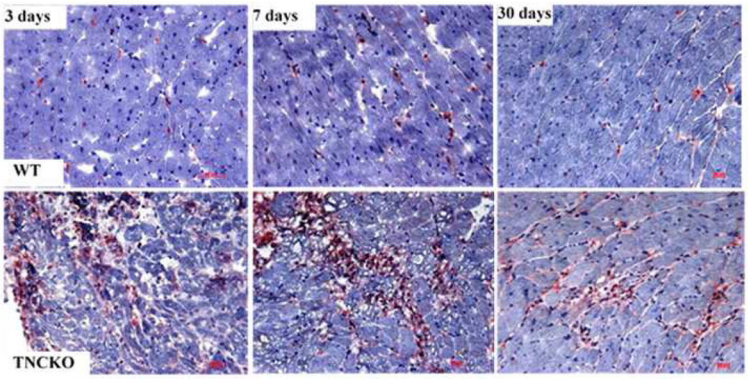

Fig. 2A

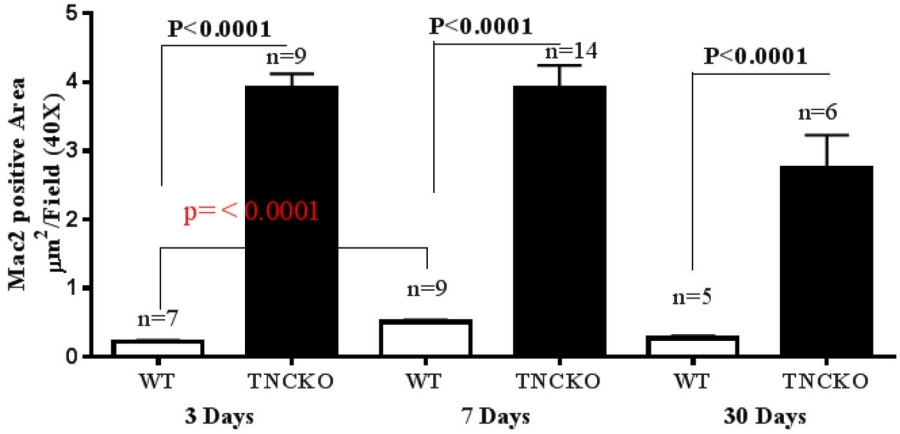

Fig. 2B

Figure 2. Leukocyte Infiltration

(**A**) Representative Mac-2 staining of sections from the LV of TNCKO and WT mice subjected to TAC show infiltration elevation and decline at 3, 7, and 30 days. (**B**) At each post-TAC timepoint, TNCKO mice had significantly higher levels of infiltration. Abbreviations as in Figure 1.

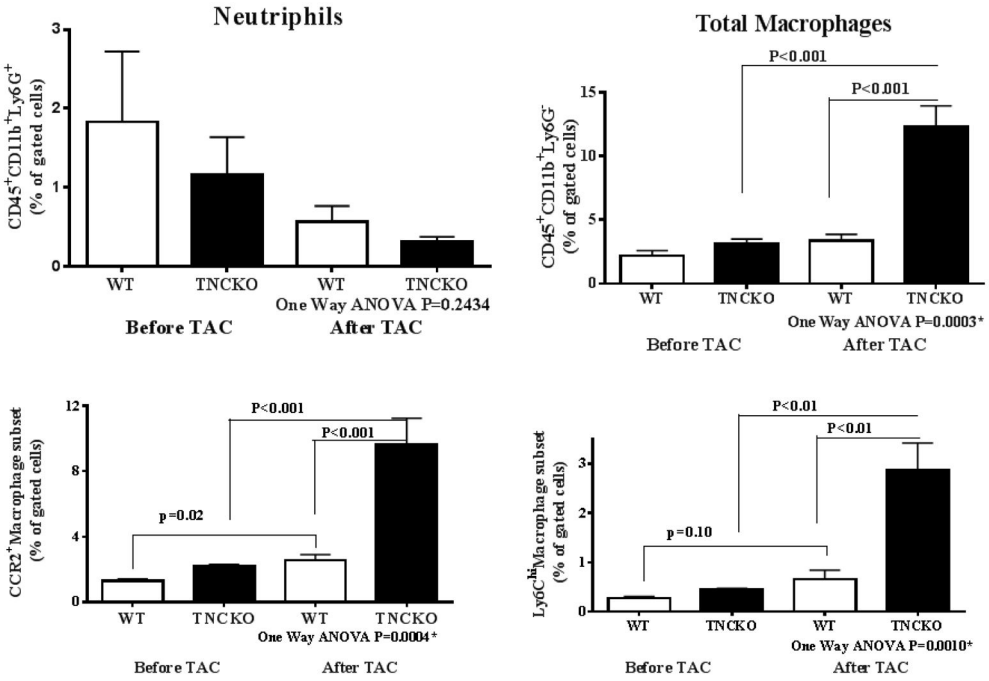

Figure 3. Proinflammatory Monocyte Infiltration

While frequency of neutrophil ($CD45^+$, $CD11b^+$, and $Ly6G^+$) infiltration was low in both 2 mice genotypes before TAC and 7 days post-TAC, TNC deficiency produced significantly greater infiltration of monocytes and macrophages post-TAC. ANOVA = analysis of variance; other abbreviations as in Figure 1.

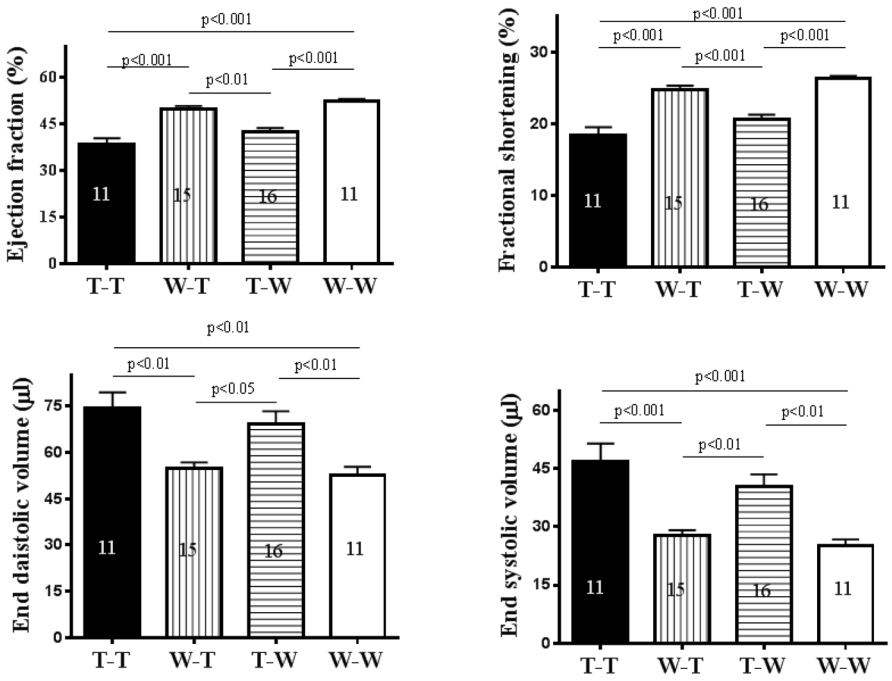

Figure 4. Bone Marrow Expression of TNC

Bone marrows were harvested from WT or TNCKO (T) donor mice and transplanted into T or WT recipient mice. In an analysis of cardiac functions, the transplantation of WT marrow significantly improved function while transplantation from TNCKO donors led to significantly worsening function. The number in each column = number of mice in each group. Abbreviations as in Figure 1.

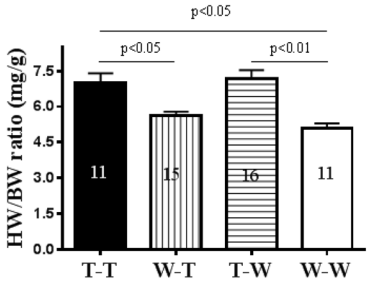

Fig. 5A

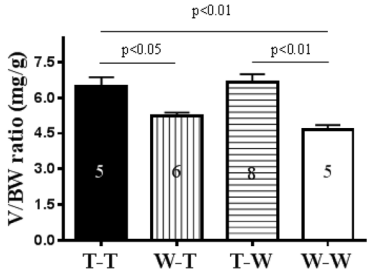

Fig. 5B

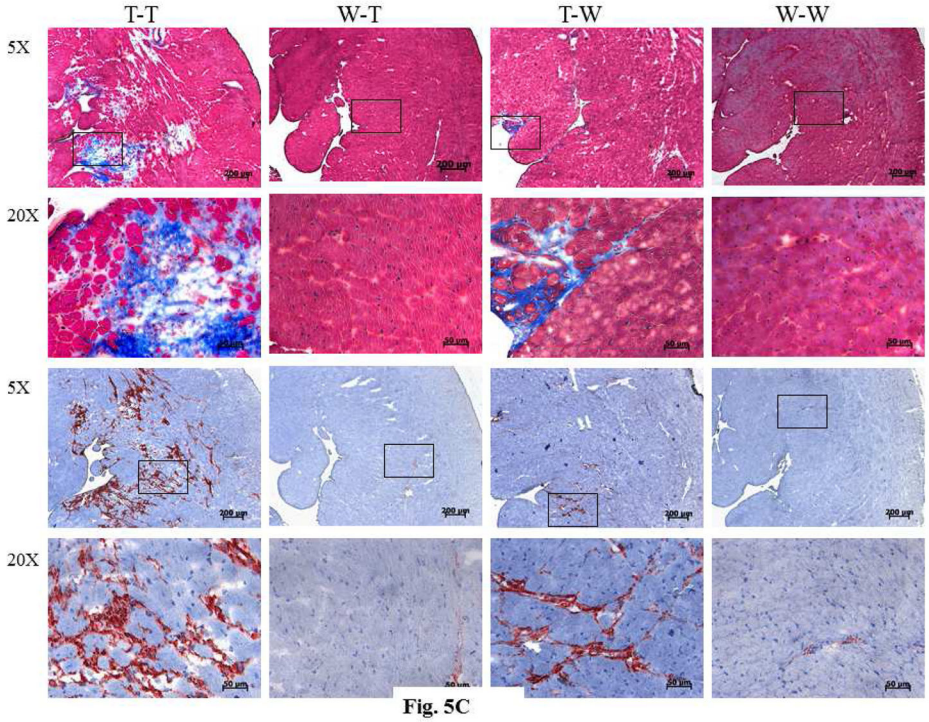

Fig. 5C

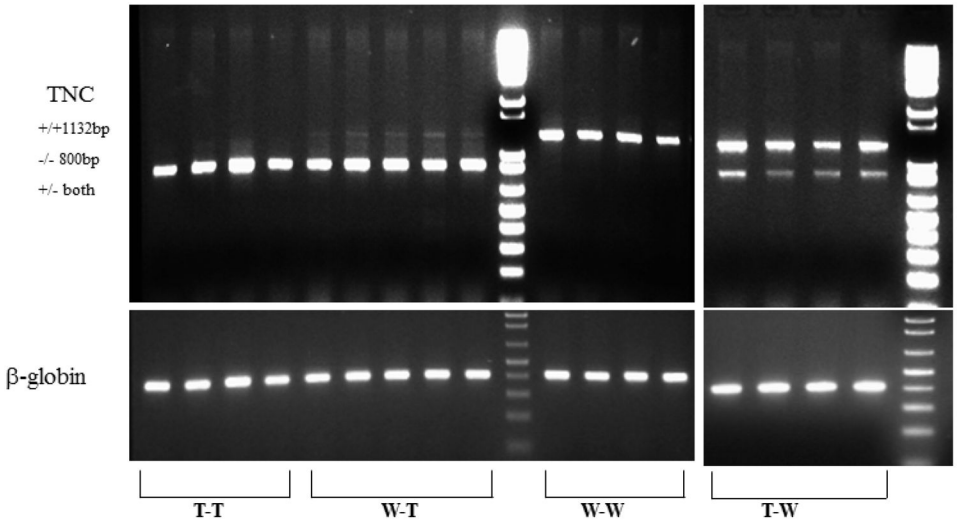

Fig. 5D

Figure 5. Analysis of the Harvested Recipient Heart

There were significant differences in the ratios of (**A**) heart weight (HW) to body weight (BW) and (**B**) heart volume (V) to BW among the bone marrow transplant groups. (**C**) As seen in immunostaining of recipient hearts, those with TNCKO donor marrow had high levels of collagen content (upper panels) and accumulation of fibroblasts (lower panels). (**D**) Genotyping of recipient hearts showed that the TNC transgene was not detectable in the TNCKO recipients but was in WT recipients. Other abbreviations as in Figures 1 and 4.

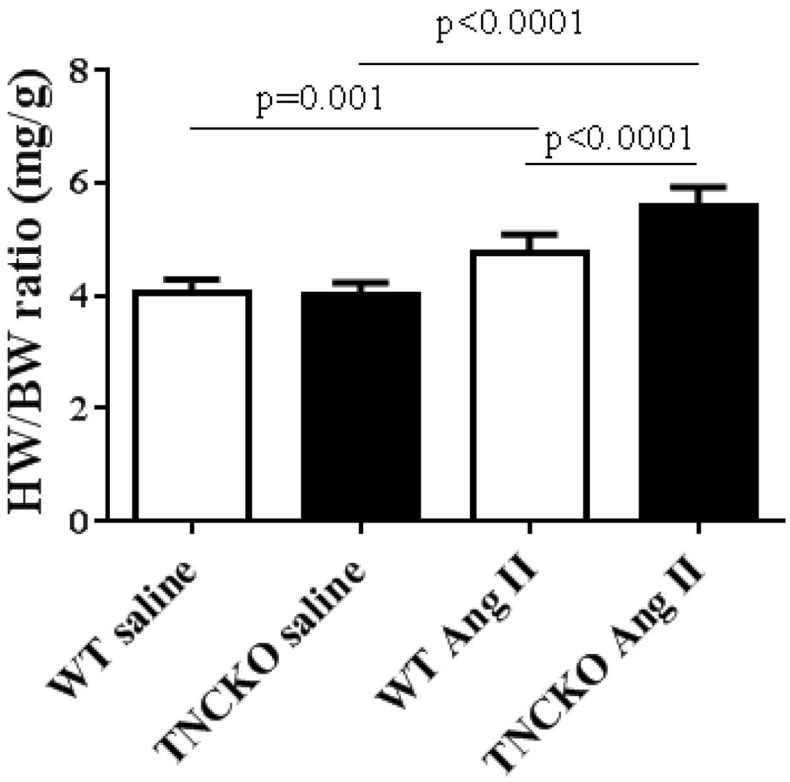

Fig. 6A

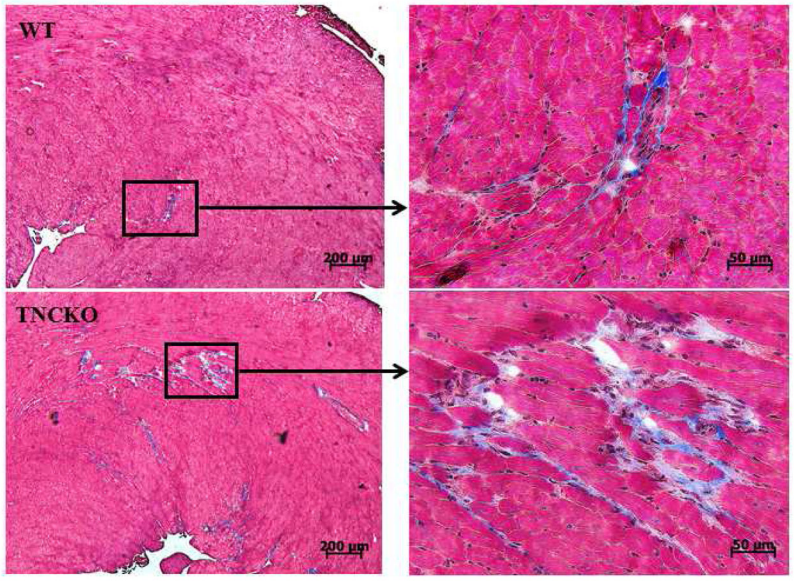

Fig. 6B

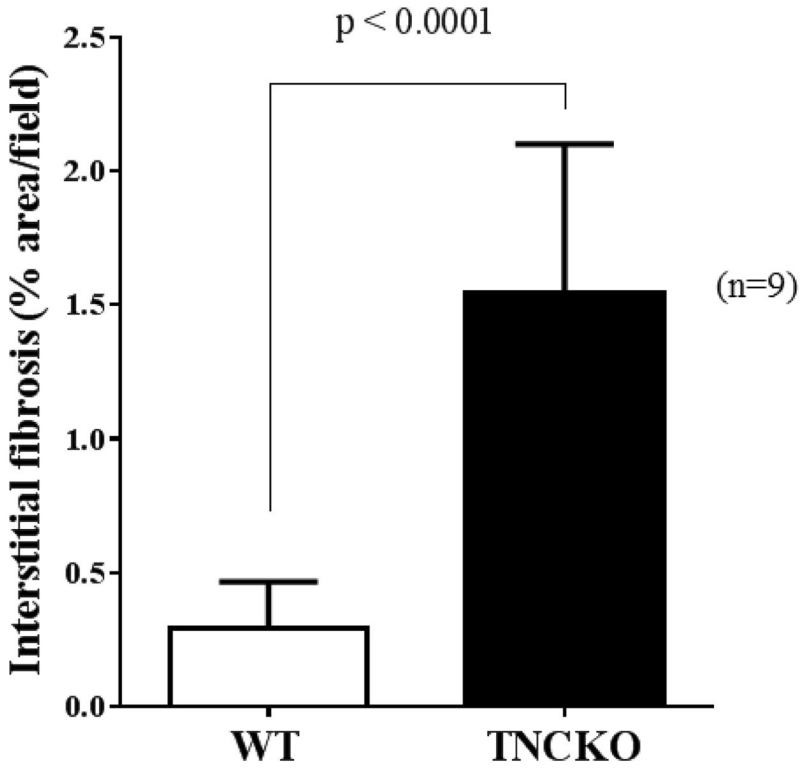

Fig. 6C

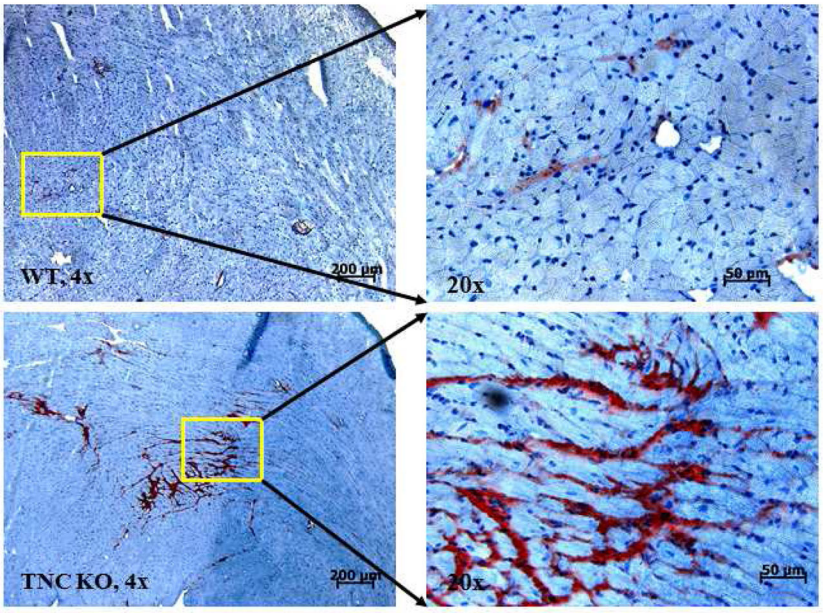

Fig. 6D

Figure 6. Effect of TNC Deficiency on AT II-induced Cardiac Hypertrophy

Infusion with angiotensin (AT) II **(A)** significantly increased HW-BW ratios but more so in TNCKO mice. As seen via immunostaining **(B)**, AT II infusion also increased collagen deposits in TNCKO compared to WT controls **(C). (D)** Similar results were seen in fibroblast frequency in peritostin-stained sections of TNCKO and WT hearts. Other abbreviations as in Figures 1 and 5.

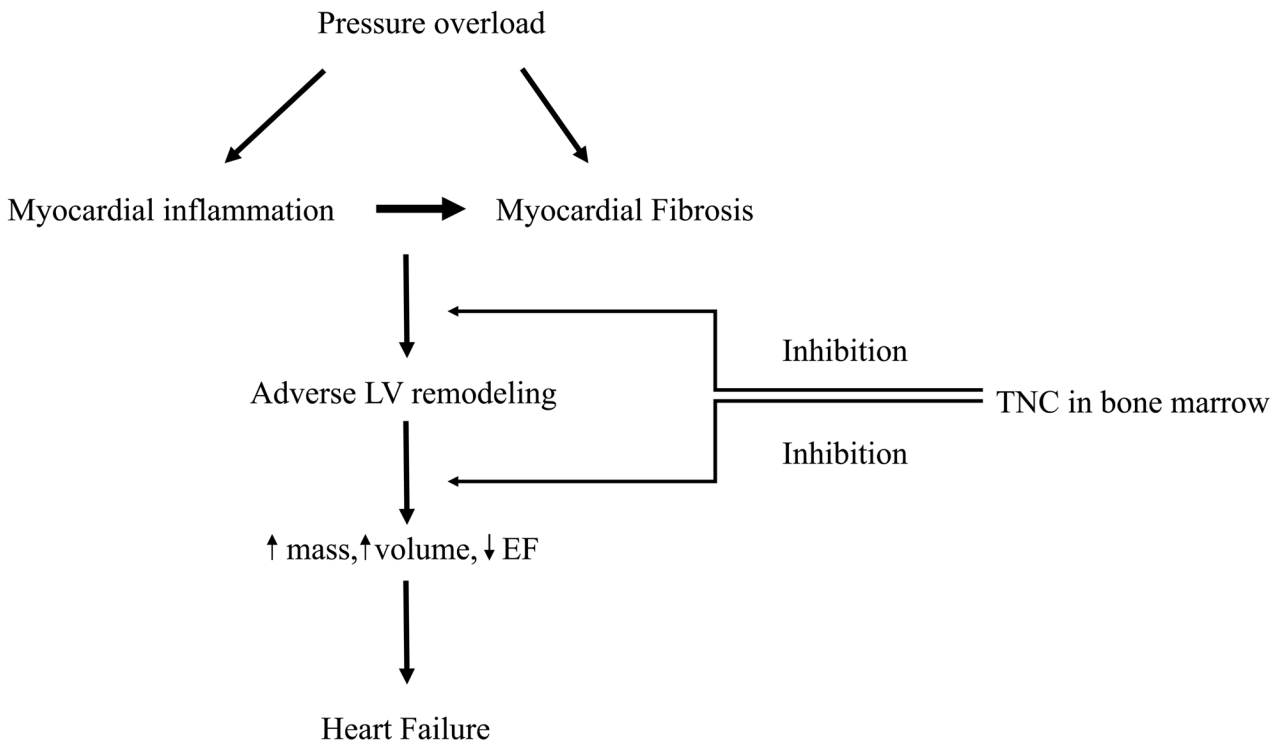

Central Illustration. Effect of TNC on Pressure Overload-induced Cardiac Remodeling

We investigated the effect of tenascin-C (TNC) deficiency on pressure overload-induced cardiac remodeling. TNC deficiency exacerbated cardiac hypertrophy and maladaptive remodeling compared to controls, by increasing the infiltration of proinflammatory monocyte subsets into the myocardium. This suggests that TNC controls excessive remodeling of the myocardium in the pressure-overloaded heart. Reciprocal bone marrow transplantation studies revealed that the expression of TNC in the bone marrow, but not myocardium, accounts for TNC's protective effect. LV = left ventricle; EF = ejection fraction.

Table 1

Echo Parameters and Heart Mass Ratio

	Wild-type			TNCKO		
	BL	**1 Month**	**2 Months**	**BL**	**1 Month**	**2 Months**
Number	16	16	8	16	16	8
Heart rate, beats/min	434 ± 34	448 ± 43	440 ± 31	436 ± 38	459 ± 34	449 ± 41
EF, %	67.2 ± 0.7	58.9 ± 2.6	51.3 ± 2.2	66.5 ± 0.6	48.9 ± 7.8 *	39.8 ± 10.6 *
FS, %	36.5 ± 0.5	30.6 ± 1.7	25.7 ± 1.3	35.9 ± 0.4	24.7 ± 4.6 *	19.5 ± 5.7 *
LVIDd, mm	3.42 ± 0.06	3.6 ± 0.18	3.65 ± 0.15	3.41 ± 0.04	4.31 ± 0.42 *	4.53 ± 0.59 *
LVIDs, mm	2.17 ± 0.05	2.51 ± 0.14	2.72 ± 0.15	2.18 ± 0.03	3.26 ± 0.48 *	3.68 ± 0.76 *
PWTd, mm	0.65 ± 0.06	0.76 ± 0.07	0.77 ± 0.1	0.67 ± 0.1	0.89 ± 0.13 *	0.93 ± 0.11 *
PWTs, mm	0.93 ± 0.09	1.09 ± 0.08	1.06 ± 0.12	0.97 ± 0.09	1.21 ± 0.14 *	1.22 ± 0.09 *
HW-BW, mg/g	3.99 ± 0.14	5.1 ± 0.09	5.5 ± 0.5	4.01 ± 0.15	6.95 ± 1.03 *	8.1 ± 1.36 *

Values are mean percent changes over baseline ± SD.

* Significant change between tenascin-C knockout (TNCKO) and wild-type mice.

BL = baseline; BW = body weight; EF = ejection fraction; FS = fractional shortening; HW = heart weight; LVIDd = left ventricular internal diameter diastolic; LVIDs = left ventricular internal diameter systolic; PWTd = posterior wall thickness diastolic; PWTs = posterior wall thickness systolic.

Table 2

Reciprocal Bone Marrow Transplantation

Mouse groups	TNC Expression: Heart	TNC Expression: Bone Marrow	Cardiac Function*
T-WT	Positive	Negative	Lower
WT-T	Negative	Positive	Higher
WT-WT	Positive	Positive	Higher
T-T	Negative	Negative	Lower

*Lower means function deteriorated and higher means it improved. The cardiac function of the positive control group (W-W) was compared to the negative control group (T-T) and vice versa, while the cardiac function of other recipient groups was compared to the similar recipient control group.

T = tenascin-C knockout; TNC = tenascin-C; WT = wild-type.

Table 3

AT II Effect on Echocardiographic Assessments and Heart Mass Ratios

	Wild-type		TNCKO	
	Saline Vehicle	**AT II**	**Saline Vehicle**	**AT II**
Number	5	9	5	9
Heart rate, beats/min	440 ± 28	426 ± 36	435 ± 18	449 ± 55
EF, %	66.6 ± 1.9	52 ± 2.5†	67.8 ± 1.6	42.8 ± 7.3*†
FS, %	36.1 ± 1.5	26.3 ± 1.6†	37.1 ± 1	20.9 ± 4*†
LVIDd, mm	3.57 ± 0.12	3.96 ± 0.23†	3.5 ± 0.28	4.08 ± 0.33*†
LVIDs, mm	2.28 ± 0.04	2.92 ± 0.16†	2.2 ± 0.18	3.23 ± 0.38*†
PWTd, mm	0.6 ± 0.07	0.77 ± 0.03†	0.64 ± 0.03	0.85 ± 0.08*†
PWTs, mm	0.92 ± 0.07	1.05 ± 0.04†	0.88 ± 0.07	1.15 ± 0.09*†
HW-BW, mg/g	4.06 ± 0.24	4.78 ± 0.4†	4.02 ± 0.21	5.26 ± 0.46*†

Values are mean ± SD.

*Significant difference between TNCKO and wild-type mice.

†Significant difference between angiotensin (AT) II treatment and saline control group.

Other abbreviations as in Table 1.